PERFORMANCE AND NEAR WAKE ANALYSIS OF A HYDROKINETIC ROTOR FOR MULTISTAGE PURPOSES USING CFD

G.A. IBARRA[1], G.L. TIAGO[2], R.G. RAMIREZ[2]

[1] Study Group in Renewable Energies, Federal University of Itajubá, Itajubá, Brazil
[2] CERPCH Executive Secretary, Federal University of Itajubá, Itajubá, Brazil
[3] Virtual Hydrodynamics Lab., Federal University of Itajubá, Itajubá, Brazil

[1] german.ibarra@unifei.edu.br, [2] tiago@unifei.edu.br, [3] ramirez@unifei.edu.br

ABSTRACT

Tidal, wave and In-stream power are new applications of renewable energy, mainly developed in advanced countries and almost unknown (or not considered) in developing countries due to high costs; the main barrier to explore and harness its potential. However, some researchers are proposing low-cost systems, as the one presented in this work called "Poraquê". This hydrokinetic system includes several low-cost axial-flow rotors in a common shaft to harness more energy from the stream. Computational Fluid Dynamics (CFD) is used to analyze its performance and near wake characteristics, in order to understand the behavior of the velocity recovery downstream of the first rotor to define a suitable separation between consecutive rotors. Results for this high-solidity rotor are in agreement with literature, besides, it was found that velocity recovers independently of the upstream velocity magnitude, i.e. separation distance to the second rotor can be defined based on velocity recovery.

Keywords: Hydrokinetic energy, low-cost turbines, efficiency gain.

INTRODUCTION

Currently, renewable energy sources are in different stages of development, since many natural resources can be used in a sustainable form in each country or region. Hydraulic energy is represented normally by conventional hydroelectric power plants based on water head, available depending the hydrological and geographical conditions of some regions in the world. However, hydraulic energy has also significant potential in water streams such as rivers, oceans and channels to extract energy. In the same way, some countries have more access to this resource and have more interest to produce large amounts of energy for attend future demand, such as the United States, China, United Kingdom (Jacobson, 2012) (OES, 2014).

Research, development and market issues have been encouraged with incentive policies in advanced countries, but high turnkey costs still remain in comparison to other renewables. Water streams, especially rivers, are spread worldwide and represent a real option to support current electricity generation: this energy is a non-polluting option with few environmental impacts (Amaral *et al*, 2012). For developing countries, this source is far to be harnessed in a large scale, then it can be used to provide lower but important electricity for population in regions without access to modern energy (GEA, 2012).

Technology development is carried out from all approaches with advances in theoretical, numerical and experimental activities. Optimization and CFD (Computational Fluid Dynamics) tools are being used for rapid improvement of hydrokinetic, tidal and wave systems. In general the pursuit of higher efficiencies is one of the goals, mainly for large-scale applications (due to its high investments), because low-cost nature influences efficiency for small-scale systems. The latter is the case of South America, where some experiences deals with the creation of small turbines for riverine applications, principally in Brazil (Anyi & Kirke, 2010). Here, we examine one of those hydrokinetic systems using CFD: a multistage turbine conceived with low-cost axial-flow rotors. One-rotor performance and near wake characteristics are analyzed to identify suitable conditions for a second rotor placement to get and efficiency gain.

2. METHODOLOGY

In this work, Computational Fluid Dynamics (CFD) involves the modeling of the Reynolds-Averaged Navier-Stokes (RANS) equations using one turbulence model, to obtain the rotor performance and flow field in the near wake in order to analyze the conditions for a second rotor placement. Commercial software ANSYS® was employed for model meshing (ICEM) and Set up (FLUENT). The system under analysis, the performance parameters and CFD aspects are described as follows.

2.1 The "Poraquê" hydrokinetic system

In theory, only 59.3% of the zero-head free-stream energy could be harnessed by some type of turbine (Betz, 1926). Most of existing systems use only one rotor, conditioning design and fabrication to a detailed and expensive process. The "Poraquê" hydrokinetic system was conceived to simplify this situation using rotors of simple geometry, placed in a common shaft. That configuration (in-series) would allow producing more energy with efficiency comparable to a more sophisticated one-rotor system.
This was found during previous experimental tests (Tiago et al, 2010), conducted on a 0.4m-width water channel where results showed an efficiency of 0.78 with 3 rotors. That efficiency exceeds Betz limit due to the blockage area ratio of 43.1% in the tests, i.e. it is known that under near-field conditions or wall effects, the performance increases (Stelzenmuller, 2013). The rotors used on tests were equal in geometry with four flat-blades and sharp corners. No hub was used. Now, it is intended to study the system performance on far-field conditions, beginning with one rotor (Fig. 1).

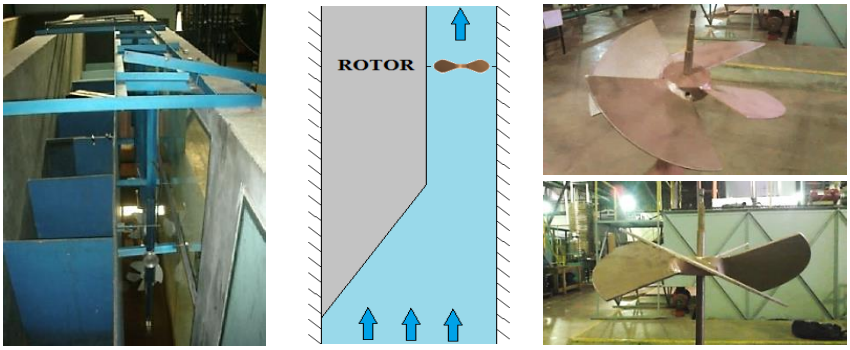

(*a*) (*b*) (*c*)

Figure 1 – Poraquê hydrokinetic system. (*a*) Experimental tests, (*b*) rotor placement during tests and (*c*) Flat-bladed rotor.

2.2 Performance parameters

Free-stream rotors, as used in wind and hydrokinetic energy, have similar design philosophy and performance characteristics (Sale *et al*, 2009). For those turbines, there are several non-dimensional coefficients to describe rotor/blade performance. Three of them, are the Tip Speed Ratio, the power coefficient and the torque coefficient, respectively (Bahaj *et al*, 2007):

$$\lambda = \frac{\omega R}{V_o} \tag{1}$$

$$C_P = \frac{T\omega}{0.5\rho A_r V_o^3} \tag{2}$$

$$C_Q = \frac{T}{0.5\rho R A_r V_o^2} \tag{3}$$

Solidity, defined as the ratio of total rotor blade area to the area swept by the rotor blades, relates inversely with λ influencing performance, torque and rotation speed. For low-λ rotors (λ *<1-2*), blade profile is large but makes the power coefficient to reduce because of rotational wake originated by drag losses and high torque (Fernandez, 1993). However, they can operate at constant C_P for a large range of λ with a high torque coefficient (Fig. 2). This is the reason for which these rotors are preferred for direct applications of shaft power (such as water pumps), and high-λ rotors for energy generation because gearbox costs decreases (Vries, 1979).

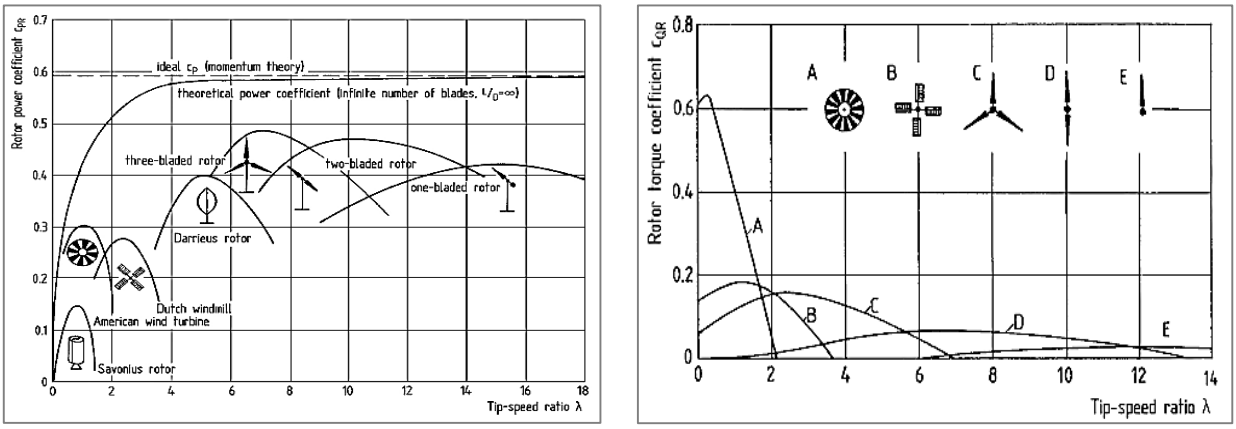

(*a*) (*b*)

Figure 2 – Performance of free-stream turbines with different solidity. (*a*) Power coefficient and (*b*) torque coefficient.

2.3 Wake behind a free-stream rotor

Free-stream turbines have some general wake characteristics and can be divided in three regions as described by Lissaman (Hau, 2006) and shown in Fig. 3. The first is the core region, just behind the rotor, where vortex structures are generated by the interaction between flow and rotor blades. Wake spin is opposite to the rotor torque to maintain the angular momentum, and the pressure begins to equalize causing wake decrease and velocity reaches its lower value between 1D and 2D. In the intermediate region, velocity rises and rotor vortices disappear gradually but significant turbulence remains after the boundary layer of the rotor wake.

In the far wake, the velocity profile turns into a Gaussian-type distribution and velocity recovers determined by turbulence intensity in the surrounding fluid. Besides of the rotational wake, the vortex structure include: the bound lift-generating vortices at the blades, the central vortex and the free-tip vortices.

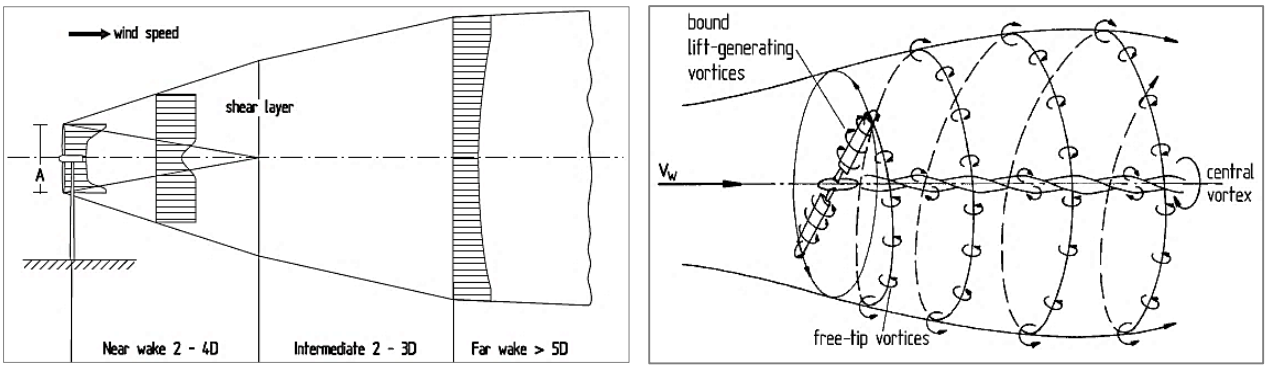

(*a*) (*b*)

Figure 3 – Rotor wake. (*a*) Model representation and (*b*) vortex system.

2.4 CFD boundary conditions and modeling

Fluid domain is a cylindrical Far-field whose dimensions are based on rotor diameters (D) to be: 3D of radius and 11D of total length. The rotor has a 3D distance upstream and 8D downstream for wake development. In this work, as in some others (Lee *et al*, 2012) (Javaherchi *et al*, 2013), this fluid domain is divided due to the symmetry in geometry and boundary conditions. Thus, the periodic boundary condition is set on the two dividing planes (Fig. 4). These features are employed to reduce processing time and computational resource.

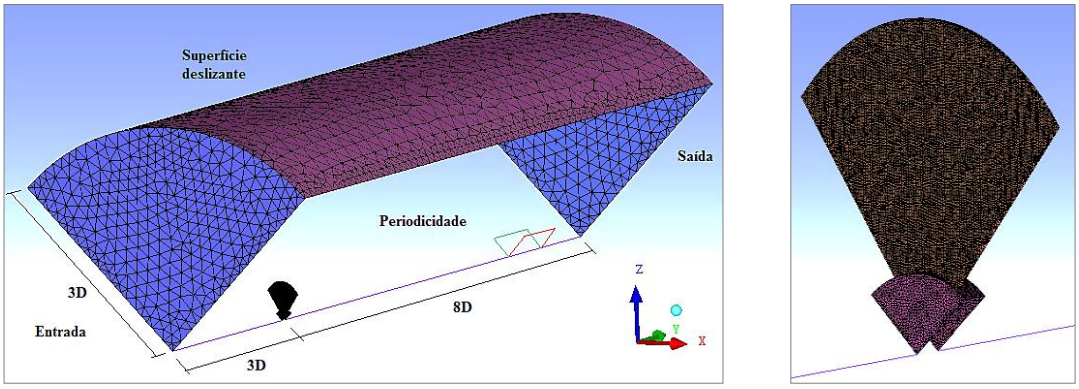

(*a*) (*b*)

Figure 4 – Fluid domain and boundary conditions. (*a*) General view and (*b*) rotor details.

Other boundary conditions on surfaces were defined as follows: a uniform velocity profile at the inlet, zero gage pressure at the outlet, an outer surface with translation speed (inlet value), and no-slip condition at rotor surfaces. The rotation was set on the rotor surfaces by means of the Single Reference Frame approach, convergence to 1E-05 and the $y^+<120$ (since SST κ-ω model works with wall functions).

Turbulence model is the SST κ-ω adding a curvature correction for streamlines, which allows capturing behavior of the free-stream (κ-ε model), the viscous effects near walls (κ- ω model) and a

more realistic near wake (Smirnov & Menter, 2009). The corresponding transporting equations in index notation for the turbulence kinetic energy and the specific dissipation rate are, respectively (Menter, 1994):

$$\frac{\partial}{\partial t}(\rho\kappa) + \frac{\partial}{\partial x_i}(\rho\kappa u_i) = \frac{\partial}{\partial x_j}\left(\Gamma_k \frac{\partial k}{\partial x_j}\right) + \tilde{G}_k - Y_k + S_k \tag{4}$$

$$\frac{\partial}{\partial t}(\rho\omega) + \frac{\partial}{\partial x_j}(\rho\omega u_j) = \frac{\partial}{\partial x_j}\left(\Gamma_\omega \frac{\partial \omega}{\partial x_j}\right) + \tilde{G}_\omega - Y_\omega + D_\omega + S_\omega \tag{5}$$

Initial values for these two turbulence variables are part of the inlet condition, which include turbulence intensity and the turbulence length scale based on rotor diameter (Minin & Minin, 2011):

$$\kappa = \frac{3}{2}(V_o I)^2 \tag{6}$$

$$\omega = \frac{\kappa^{1/2}}{C_\mu^{1/4}\, l} \tag{7}$$

2.3 Validation

Validation is to be made over Best efficiency point when comparing experimental with CFD results. However, in tests conditions the blockage area ratio of 43.1% is larger than recommended (Ibarra & Palacios, 2013) and generates wall effects over results. Therefore, these values must be equalized to the same conditions in order to make the comparison possible. To overcome this situation, the experimental coefficient ($C_{P,ch}$) is transformed to its far-field equivalent ($C_{P,f}$) using the following equation (Bahaj *et al*, 2007):

$$C_{P,f} = C_{P,ch}\left(\frac{V_{ch}}{V_f}\right)^3 \tag{8}$$

Additionally, CFD results can be verified using similitude laws for turbomachines considering constant efficiency data for the following variables (Dixon, 1998):

$$\frac{Q_2}{Q_1} = \left(\frac{\omega_2}{\omega_1}\right)\left(\frac{D_2}{D_1}\right)^3 \tag{9}$$

$$\frac{P_1}{P_2} = \left(\frac{\omega_2}{\omega_1}\right)^3\left(\frac{D_1}{D_2}\right)^5\left(\frac{\rho_2}{\rho_1}\right) \tag{10}$$

With equal diameters, they are finally simplified to,

$$\frac{V_2}{V_1} = \frac{n_2}{n_1} \tag{11}$$

$$\frac{T_2}{T_1} = \left(\frac{n_2}{n_1}\right)^2 \tag{12}$$

3. RESULTS AND DISCUSSION

3.1 Rotor performance

Rotors with high-solidity, as in this case (85.87%), show a relative low performance and higher torque coefficient as a function of Tip speed ratio. CFD results present maximum values of 0.222 (λ = 1.230) and 0.335 (λ = 0.291) for power and torque coefficients, respectively (these values do not correspond to maximum of regression curves). Besides, power coefficient remains almost constant for several inflow velocities and rotation speeds (Table 1) as mentioned in section 2.

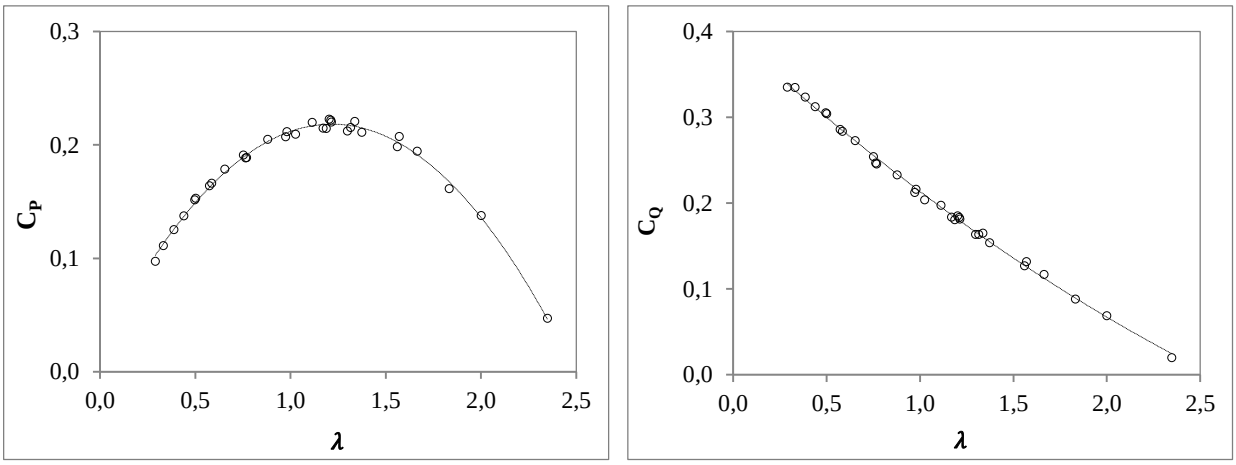

(*a*) (*b*)

Figure 5 – Rotor performance. Curves of (*a*) CP – λ and (*b*) CQ – λ.

Table 1 – Conditions assuming constant efficiency (C_P).

V [m/s]	n [rpm]	C_P	ΔC_P	P [W]
1,17	90,39	0,214	0,003	12.44
1,50	114,64	0,217	-	25.81
1,75	137,07	0,216	0,001	42.11
2,00	151,03	0,208	0,009	60.67

For results validation, values for maximum power coefficient in experimental and numerical results are compared. Using Eq.8, the corresponding far-field equivalent for water channel test (0.340) is 0.168 (Tiago *et al*, 2010). The difference with numerical value of 0.222 can be explained by the instabilities conditions during tests, i.e. the non-uniform velocity profile upstream rotor due to the asymmetric converging section and rotor placement from it. Similitude laws (Eq.11, Eq.12) were verified using CFD results assuming constant efficiency in Table 1. The values for lowest velocity were considered reference for the rest (Fig. 6).

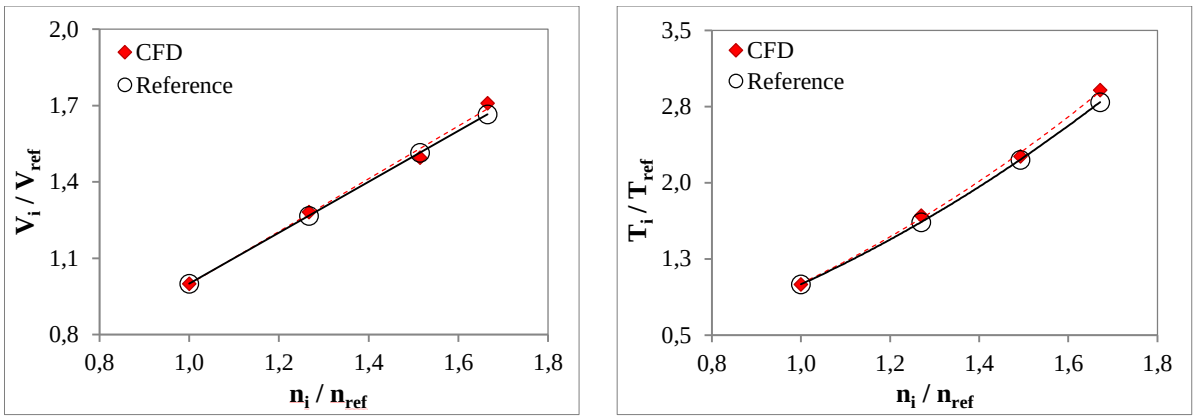

(*a*) (*b*)

Figure 6 – Similitude laws verified for the rotor. (*a*) Linear relation in Eq.11 with R^2=0.9935, and (*b*) quadratic relation in Eq.12 with R^2=0.9987.

3.2 Rotor wake

Velocity contours at midplane in Fig. 7 show the wake development with a gradual velocity recovery, taking more than 8D as in other works in literature (Bahaj, 2011) (Tedds *et al*, 2014). This can be quantified at centerline (y/D = 0) in Fig. 8a for each velocity. If these data is non-dimensionalized, it can be noted that velocity recovers quantitatively 24.4% at 1D, 10.1% at 2D, 31.4% at 3D, 48.9% at 4D, 57.9% at 5D, 64.5% at 6D, 67.8% at 7D and 70.2% at 8D (Fig. 8b).

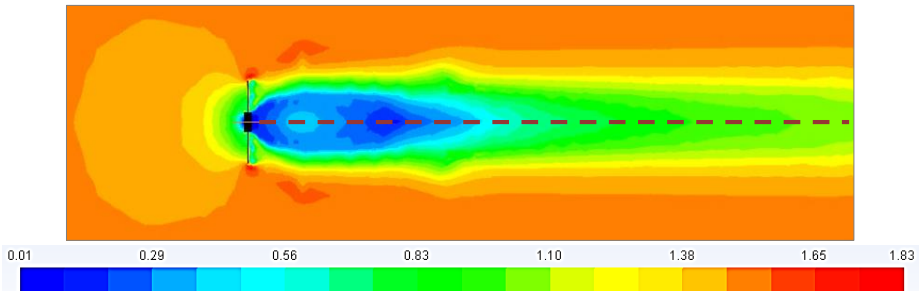

Figure 7 – Contours of velocity magnitude at midplane (Dashed line: Centerline)

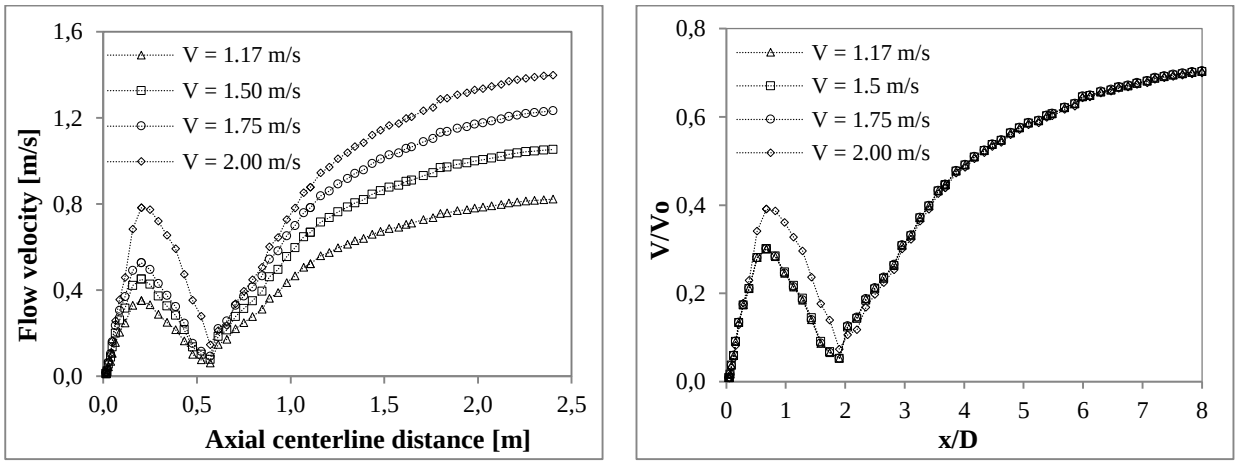

(*a*) (*b*)

Figure 8 – Velocity recovery at centerline. (*a*) Dimensional and (*b*) non-dimensional values.

From Figure 8b, it can be seen two main aspects: first, the minimum velocity is between 1D and 2D as mentioned in theory (section 2.3); second, velocity recovery is practically independent of flow velocity upstream rotor. This means, second rotor can be placed at some distance depending on the percentage of velocity recovery. Differences for the higher velocity could be related to Reynolds number effects.
For other hand, the turbulence structures described in theory are represented by the streamlines: the rotor wake, tip vortices and central vortex are represented using SST κ-ω and curvature correction (Fig. 9). These vortex structures are influenced by rotor solidity and the poor rotor/blade hydrodynamics, i.e. blades with sharp corners and without a proper profile, as well as the absence of a nacelle (nose/ogive).

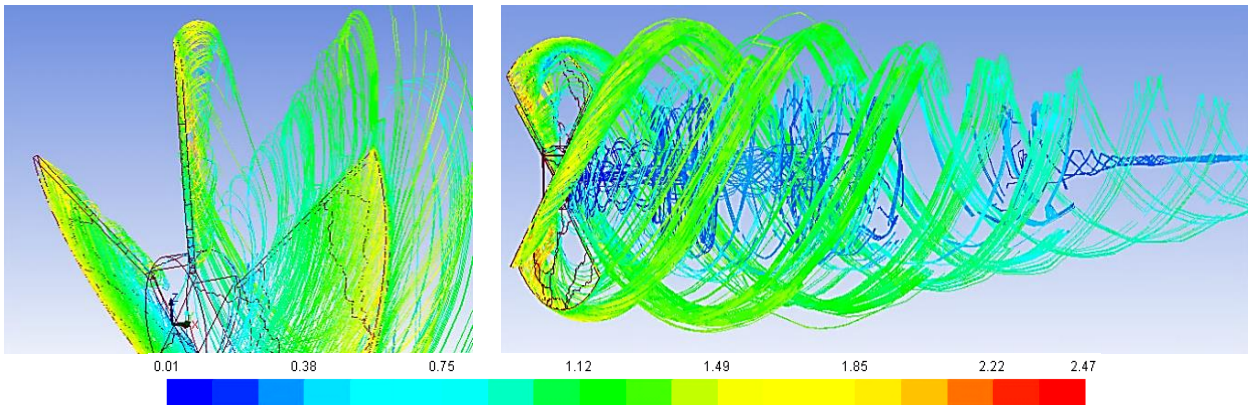

Figure 9 – Streamlines released from rotor showing main vortex structures in the wake.

4. CONCLUSSIONS

This work presents some results from the CFD modeling of a hydrokinetic turbine. The fluid domain was simplified, using just one-quarter of the cylindrical Far-field. Performance, described here with power and torque coefficient, is according with literature based on the solidity (85.87% for this rotor), i.e. low-λ curves ($0.291 < \lambda < 2.35$) for C_P (0.222 max.) and C_Q (0.335 max.). However, these values are generated by not suitable hydrodynamics: a rotor without a blade profile and a complete nacelle/ogive.
Wake was also analyzed. Velocity contours show the field recovery along downstream distance, which is gradual except for the minimum velocity region between 1D and 2D as described in theory. Non-dimensionalized results for velocity recovery at centerline (shaft) present a behavior independent from upstream velocity: this means that second rotor separation would not be changed with that velocity, just with the velocity recovery to be harnessed. For other hand, streamlines represent the main vortex structures in the wake, derived from de use of the SST κ-ω turbulence model with the curvature correction factor available in the software.

5. ACKNOWLEDGMENTS

The authors would like to thank Brazilian institution CAPES for funding the main research, from which this works is part of.

NOMENCLATURE

A_r	Rotor swept area	m^2
C_P	Power coefficient	---
C_Q	Torque coefficient	---
C_μ	Constant	---
D	Rotor diameter	m
D_ω	Cross diffusion term	Kg/m^3s^2
$\bar{G}_k$, $\bar{G}_\omega$	Production terms of κ and ω	$Kg/m.s^3$, Kg/m^3s^2
I	Turbulence intensity	%
P	Shaft power	W
Q	Rotor Flow rate	m^3/s
R	Rotor radius	m
S_k , S_ω	Source terms of κ and ω	$Kg/m.s^3$, Kg/m^3s^2
T	Shaft torque	N.m
V_o	mean upstream velocity	m/s
V_f	Velocity in free-stream condition	m/s
V_{ch}	Velocity in water channel tests	m/s
Y_k , Y_ω	Dissipation terms of κ and ω	$Kg/m.s^3$, Kg/m^3s^2
l	Turbulence length scale	m
Γ_κ , Γ_ω	Effective diffusivity of κ and ω	Kg/m.s , Kg/m^2s
λ	Tip Speed Ratio	---
κ	Turbulence kinetic energy	m^2/s^2
ρ	water density	Kg/m^3
ω	Angular velocity, specific dissipation rate	rad/s, 1/s

REFERENCES

Amaral S V, Castro-Santos T, Giza D, Haro A J, Hecker G, McMahon B, Perkins N and Pioppi N 2012 *Environmental Effects fo Hydrokinetic Turbines on Fish: Desktop and Laboratory Flume Studies: Tech. Report EPRI (*Palo Alto, USA: EPRI) *(EPRI Electric Power Research Institute)*

Anyi M and Kirke B 2010 Evaluation of small axial flow hydrokinetic turbines for remote communities *Energy Sustain. Dev.* **14** 110-6.

Bahaj A S 2011 Generating Electricity from the oceans *Renew. Sustain. Energy Rev.* **15** 3399-416

Bahaj A S, Molland A F, Chaplin J R and Batten W M j 2006 Power and thrust measurements of marine current turbines under various hydrodynamic flow conditions in a cavitation tunnel and a towing tank *Renew. Energy* **32** 407-26

Betz A 1926 Windenergie und ihre Ausnutzung durch Windmuhlen (Göttingen: Vandenhoeck und Ruprecht).

Dixon S L 1998 *Fluid mechanics and thermodynamics of turbomachinery* (Sidney: Elsevier Butterworth-Heinemann)

Fernandez P 1993 *Energia Eolica* (Santander, Espanha: Servicio Publicaciones E.T.S.I. Industriales y T.)

GEA 2012 *Global Energy Assessment: Toward a Sustainable Future* (Cambridge: Cambridge Univ. Press, USA).

Hau E 2006 *Wind Turbines: Fundamentals, Technologies, Applications, Economics* (Berlin: Springer)

Jacobson P 2012 *Assesment and Mapping of the Riverine Hydrokinetic Energy Resource in the Continental United States: Tech. Report EPRI (*Palo Alto, USA: EPRI) *(EPRI Electric Power Research Institute)*

Javaherchi T, Stelzenmuller N and Aliseda A 2013 *Experimental and Numerical Analysis of the Doe Reference Model 1 Horizontal Axis Hydrokinetic Turbine: Proc. of the 1st Marine Energy Technology Symposium METS13* (Washington, D.C., EEUU, 10-11 April 2013).

Lee J H, Park S, Kim D H, Rhee S H and Kim M C 2012 Computational methods for performance analysis of horizontal axis tidal stream turbines *Appl.Energy* **98** 512-23

Menter F R 1994 Two-Equation Eddy-Viscosity Turbulence Models for Engineering Applications *AIAA Journal* **32** 1598-605

Minin I and Minin O 2011 *Computational Fluid Dynamics Technologies and applications* (Croatia: InTech).

Ocean Energy Systems 2014 *Worldwide Database for Ocean energy: GIS mapping application* http://www.ocean-energy-systems.org/ocean_energy_in_the_world/gis_map/

Sale D, Jonkman J and Musial W 2009 *Hydrodynamic optimization method and design code for stall-regulated hydrokinetic turbine rotors: ASME 28 Int. Conf. on Ocean, Offshore and Artic Eng. (Honolulu, USA, 11 May – 5 June 2009) (National Renewable Energy Laboratory, NREL/CP-500-45021)* pp 1–17.

Smirnov P E and Menter F R 2009 Sensitization of the SST Turbulence Model to Rotation and Curvature by Applying the Spalart-Shur Correction Term J. Turbomach T ASME 131(4) 040410

Tiago G L, Silva F G B, Barros R M, Silva F das G B 2010 “Poraquê” hydrokinetic turbine *IOP Conf. Series Earth Environ. Sci.* **12** (2010) 012094.

Tedds S C, Owen I and Poole R J 2014 Near-wake characteristics of a model horizontal axis tidal stream turbine *Renew. Energy* **63** 222-35

Vries O de 1979 *Fluid Dynamic Aspects of Wind Energy Conversion* (Amsterdm: Advisoroy Group for Aerospace Research and Development AGARD)